

## Receiver Design of Passive UHF RFID Sensor Platform for Gas Identification

Muhammad Ali Akbar, Amine Ait Si Ali, Abbas Amira, Mohieddine Benammar, Faycal Bensaali  
College of Engineering  
Qatar University  
Doha, Qatar  
e-mail: ali.akbar@qu.edu.qa,  
amine.aitisali@qu.edu.qa,  
abbes.amira@qu.edu.qa,  
mbenammar@qu.edu.qa,  
f.bensaali@qu.edu.qa

Mohamed Zgaren, Mohamad Sawan  
Dept. of Electrical Engineering  
Polytechnique Montreal  
Montreal, Quebec  
e-mail: mohamed.zgaren@polymtl.ca,  
mohamad.sawan@polymtl.ca

Amine Bermak  
School of Engineering  
Hong Kong Uni. of Sci. and Tech.  
Clear Water Bay, Hong Kong  
e-mail: eebermak@ust.hk

**Abstract**— The concept of passive Radio Frequency Identification (RFID) sensor tag is introduced to remove the dependency of current RFID platforms on battery life. In this paper, a reader for passive RFID sensor tag is presented along with the processing unit. The RFID system is compliant to Electronics Product Code Generation 2 (EPC-Gen2) protocol in 902-928 MHz ISM band. Whereas the processing unit is implemented and analyzed in software and hardware platforms. The software platform uses MATLAB, whereas a High Level Synthesis (HLS) tool is used to implement the processing unit on a Zynq platform. Moreover, Principal Component Analysis (PCA) and Linear Discriminant Analysis (LDA) based feature reduction approaches are analyzed in detail for efficient classification of gas data. It is found that 90% gases are identified using first three principal components, which is 7% more efficient than LDA. While in hardware, LDA requires 50% less Look-Up Tables than PCA. The RFID tag used for transmission is implemented in 0.13  $\mu\text{m}$  CMOS process, with simulated average power consumption is 2.6  $\mu\text{W}$  from 1.2 V supply. ThingMagic M6e embedded reader is used for RFID platform implementation. It shows an output power of 31.5 dBm which allows a read range of 9 meter.

**Keywords**—Sensor tag; Pattern recognition; Gas identification; UHF RFID Reader; EPC Gen2; ISM Band

### I. INTRODUCTION

Gas identification is one of the most critical challenges in current gas industry because a single leakage of an explosive gas can cause a complete disaster for the whole company. The explosion of a gas container or the leakage of a hazardous gas will also be disastrous for the environment [1]. Therefore, human olfactory based Electronic Nose (EN) systems are introduced, with wide range of applications like milk industry [2] and patient monitoring system [3].

In gas applications, the presence of complex compounds like water vapour with the gases of interest creates one of the challenging issues for the gas identification using EN [4]. The presence of battery further limits the life and durability of the sensor tag. Moreover, the drift and non-selectivity of sensor raise the problem of classification for EN [5]. The possible approaches to deal with the problem of drift and non-selectivity is to increase the number of sensors as adopted by Guo et al. [6] or to introduce the temperature modulation such that a single sensor provides different responses for the same gas due to temperature variations [7]. The purpose of these approaches

is to get more signatures for the same gas, whereas both approaches of multiple-sensors and single sensor-modulation increase the dimensionality of feature vector, thereby increasing the computational complexity. The problem becomes severe if the gas identification system is implemented on any hardware platform because of resource utilization and power consumption which increases with the computational complexity. Therefore, feature reduction approaches like Principal Component Analysis (PCA) or Linear Discriminant Analysis (LDA) is required to reduce the data size and to increase the processing efficiency.

On the other hand, Radio Frequency Identification (RFID) sensing design has been widely explored as a low-cost candidate toward lightweight, reliable and energy-efficient devices for gas detection [8]. There has been permanent evolution toward combining the capabilities of gas sensing and wireless technology in order to collect, process, and transmit time-varying data. This approach leads to RFID-enabled Wireless Sensor Network (WSN) infrastructure. Most of the WSN include a battery [9], which increases their cost and limits their autonomy. The power autonomy can be encountered by using a fully passive (battery-less) UHF RFID design. A typical RFID system is mainly composed by a reader and antenna (also named interrogator), one to several tags (also named electronic labels) and an information systems back-end.

Furthermore, a reconfigurable hardware is required to improve the processing time for run-time classification because a dedicated hardware is faster than the software application. However, gas recognition process requires a complicated training phase and frequent calibration, which is even harder to implement on a dedicated hardware. As a consequence, most EN solution today are software based platforms and the integration of a real-time in-site training and portable EN microsystem is yet to be demonstrated. Therefore, a hardware based processing unit is demonstrated which can be applied in any multi-sensing gas identification platform. The presence of a processor along with a programmable logic based on field programmable gate array (FPGA) has made heterogeneous Zynq platform suitable for our research. A hybrid system can easily be implemented on Zynq using High Level Synthesis (HLS) tool. The other reason for using Zynq board is because the circuit implemented and tested on it can easily be reproduced to application-specific integrated circuit (ASIC).

Therefore, in this paper the reader for a passive Ultra-High Frequency (UHF) RFID sensor platform is presented with a

centralized hardware processing unit to perform feature reduction and classification. The data from multiple sensor tags will be collected using M6e embedded reader at the central processing unit with respect to the Electronics Product Code Generation 2 (EPC-Gen2) protocol in the 902-928 MHz ISM frequency band. Each sensor tag has a 4x4 array gas sensor proposed by Guo et al. [6] and a low power temperature sensor [10]. Moreover, a unique code is associated with all sensor tags individually which helps the processing unit to identify the tag and process the collected data accordingly. The central processing unit is tested on a heterogeneous reconfigurable Zynq platform using High-Level Synthesis (HLS) tools while the tag sensors are implemented in CMOS process to reduce the power dissipation and enhance the full system integration. The presented work is part of an ongoing project in which a low-power multi-sensing gas identification platform is need to be developed for gas identification based on an array of tin-oxide gas sensors.

The remaining sections of this paper are organized as follows. Section II covers the RFID sensor tag along with the experimental setup for data acquisition. The UHF RFID receiver is described in Section III. Section IV is concerned with the processing unit. Simulation results are shown and discussed in Section V. Section VI concludes the paper.

II. RFID SENSOR PLATFORM AND DATA EXTRACTION

The UHF RFID based sensor platform includes a 4x4 array gas sensor [6] and a low power temperature sensor [10]. The main challenge of the RFID sensor design is the power hungry building blocks for which an external power source is required. Whereas, the presence of battery in the sensor tag creates problems by limiting the lifetime of the tag-based sensors. Tags will not be able to communicate with the embedded reader if battery power level goes below a fixed threshold. Therefore, a fully passive UHF RFID approach is adopted such that, the communication link between tags based sensor and reader is guaranteed for longer time. The full tags based sensor system are powered by a remote power through the RF energy received from the reader in order to create autonomous gas measurement micro systems.

The main challenge with the passive RFID tag is the limited range of communication; therefore, hybrid design could be used by adding a battery as power bank in addition to the power harvesting circuit. The power bank will allow to reach higher communication range when needed. Furthermore, 16 gas sensors are used in the tag which results in huge

transmission overhead as tag needs to transmit the data in periodic sessions which in turn further increases the problem of power consumption, therefore a compressive sensing approach such as Orthogonal Matching Pursuit (OMP) algorithm can be adopted for reconstructing the compressed signal [11].

In order to test the sensor tag, data is extracted for 10 concentrations of 20, 40, 60, 80, 100, 120,140, 160, 180 and 200 ppm in air, of three different gases namely Carbon-mono-oxide, ethanol and hydrogen, in a controlled experimental environment. The extraction process of gas data is carried out in a way that the dry air is flushed for 750 s before exposing the sensor to any new concentration of gas. The sensor is then exposed to gas for 250s in a closed glass chamber. This is due to the fact that the sensor reaches steady state after 250s. The experiment is repeated again after obtaining the data for 10 concentrations of each gas such that the obtained data is divided into two parts. The first one is used for training purpose known as learning data ( $D_l$ ) and the second one for testing purpose known as test data ( $D_t$ ). The overall model of sensor tag is shown in Figure 1.

III. UHF RFID READER PERFORMANCE

A typical RFID system consists of tags, readers and computer application systems, as shown in Figure. 2. With several excellent characteristics, such as portable, high capacity, long life, security access, and movable recognition, RFID is used more and more widely in logistic systems, production management system, monitoring and tracking system, and so on [12]. The EPC Gen2 protocol was designed based on the minimal features available on an EPC Gen2 RFID tag specifically a 32-bit secret access password, a 16-bit pseudo-random number generator, and limited memory that can store at least two 16-bit random numbers while the tag is powered. An improved authentication scheme is adopted with this standard [13].

The communication range performance of a RFID system depends mainly on the choice of frequency, transmitted power from the reader, sensitivity of tag, tag’s modulation efficiency, data rate, reader receiver sensitivity and location of the tag [14]. Based on the frequency, the RFID system can be considered as Low Frequency (LF), High-Frequency (HF), UHF and Microwave (WF) RFID. Nowadays, the UHF RFID is the most used technology because of its far reading distance (up to 10 meter), passive (battery less) tags, high security, and strong penetrating force features [15].

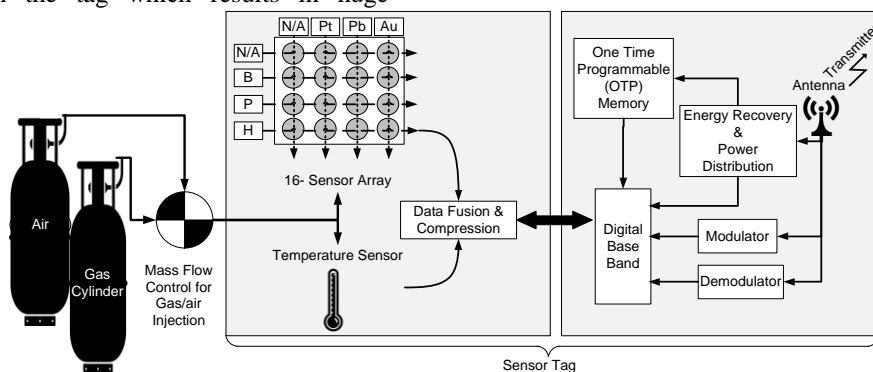


Figure 1. Block Diagram of RFID Sensor tag with data acquisition set-up

As shown in Figure. 2, the controller activates the RFID reader to send RF signals. Tags receive, process and send back the requested data through the tag’s antenna. The tag responds with an identification code using backscattering of modulated received signal. There is no battery as source of energy in the passive tags system, and thereby it gets all the energy needed for running from the electromagnetic wave transmitted by the reader. The reader decodes the received signal through its antenna to be processed by the controller.

In most cases, the reader’s antenna is placed into an external module as presented in Figure. 2 to achieve long read/write ranges also when a circularly polarized reader antenna is used to eliminate tag orientation sensitivity. According to different configurations and parameters , UHF RFID readers can be designed as fixed or handheld readers.

Handheld readers are used in a large number of applications for its portable, and easy to use in shift data collection. It is complicated to design handheld UHF RFID reader, while it includes embedded computer middleware and application, microwave and antenna designs, radio frequency electronic circuits, wireless communications and signal processing, low-power control and many other technical fields. In this research, embedded RFID reader is taken into consideration to reduce the overall system cost and complexity.

A. Antenna Design

Among the important performance characteristic is the maximum range at which RFID reader can detect the backscattered signal from the tag. Because reader sensitivity is typically high in comparison with tag, the reading range is defined by the tag response threshold. Communication range is also sensitive to the tag orientation, the material the tag is placed on, and to the propagation environment. The reader antenna should be a circularly polarized antenna, in order to avoid the polarization loss when the orientation of the identified object is changed. The read range  $r$  can be calculated using Friis free-space formula as:

$$r = \frac{\lambda}{4\pi} \sqrt{\frac{P_t G_t G_r \tau}{P_{th}}} \tag{1}$$

where  $\lambda$  is the wavelength,  $P_t$  is the power transmitted by the reader,  $G_t$  is the gain of the transmitting antenna,  $G_r$  is the gain of the receiving tag antenna,  $P_{th}$  is the minimum threshold power necessary to provide enough power to the RFID tag chip, and  $\tau$  is the power transmission coefficient.

B. Link budget

In UHF RFID systems, the forward link depends on the tag sensitivity  $P_{tag}$  while the return link depends on the reader sensitivity  $P_{reader}$ . The reader can process the tag response data when the tag signal power  $P_r$ , received at the reader, is larger than the reader sensitivity. The reader sensitivity is the minimum power of the received tag signal necessary for successful data processing and is mainly defined by the level of self-jammer [16]. One important characteristic is the needed reader sensitivity to detect an arbitrary tag at the maximum possible distance. From [16], the needed reader sensitivity must be better or equal to:

$$P_{reader} = \frac{P_{tag}^2 * K}{P_t} \tag{2}$$

Where  $K$  is the tag backscatter gain and  $P_t$  is the reader output power. The given equation is valid for any propagation environment. Figure. 3 shows the reader sensitivity requested by the tags to read command at their maximum possible range [16]. The backscatter gain is assumed to be -10dB. The study illustrated in Figure. 3 uses four readers with four levels of output power 30dBm, 20dBm, 10dBm and 0dBm.

C. ThingMagic M6e embedded RFID reader

To further verify the performance of the proposed UHF tag [17] for both near-field and far-field operations, the Thing Magic M6e embedded RFID reader module [18] is studied to be used with a circularly polarized antenna in the free space. This RFID reader module supports the ability to transmit up to 31.5dBm for the UHF RFID band of 902–928MHz and can read more than 750 tags/seconds. This performance makes M6e the recommended RFID reader for challenging applications such as gas identification and temperature monitoring. The M6e has both serial and USB interfaces to support both board-to-board and board-to-host connectivity.

The maximum tags read range can reach up to 30 feet (9 meters) for an operating temperature from -40 °C to 60 °C.

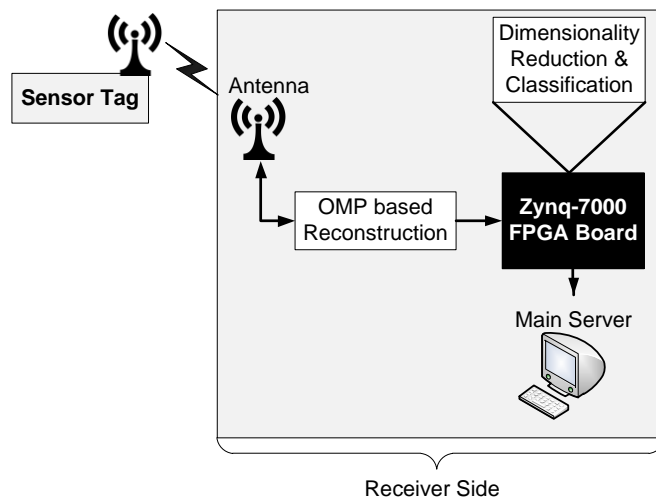


Figure 2. RFID System architecture diagram



Figure 3. Reader sensitivity comparison at -10dB backscatter gain

IV. PROCESSING UNIT

The data received by the RFID receiver is fed to the processing unit for analysis. The possibility of parallel computation in dedicated hardware makes it much faster than the software at run-time. Therefore the processing unit is implemented on heterogeneous reconfigurable Zynq platform which is having an ARM processor and FPGA chip based on Xilinx 7-series [20]. The reason of selecting the Zynq platform is because of its suitability for hardware/software co-design approach. It is worth noting that the purpose of hardware platform is to process the  $D_i$  whereas the training part is done offline using MATLAB. This is to reduce the hardware overhead caused by the complexities of the feature reduction and classification algorithms. Also, the  $D_i$  is used one time for training purpose so it is more feasible and efficient to do the training offline. Thus, the hardware processing unit is used to perform real-time feature reduction and classification on  $D_i$  of gases.

A. Compressive Sensing Reconstruction

The data acquired by the sensor is compressed before transmission to reduce the power overhead of sensor tag required for transmission purpose. After receiving the RFID signal the processing unit should need to reconstruct the compressed signal to acquire the original sensor data. There are different approaches for reconstruction process, however in this research we utilized the OMP based reconstruction algorithm proposed in [11]. The reason of using this algorithm is due to its scalability and high Peak Signal to Noise Ratio (PSNR).

B. Feature Reduction

After reconstruction a PCA and LDA based feature reduction approaches are applied to check the suitability of the two most common reduction algorithms for gas application. The aim of feature reduction is to reduce the feature size without losing useful information. PCA and LDA-based feature reduction algorithms are summarized in Figure. 4.

In case of PCA the Eigen vectors ( $E_v$ ) and mean values will be computed offline for training data  $D_i$  and then the projection of  $D_i$  in new space is obtained by simple multiplication of normalized data with the  $E_v$  using MATLAB. Whereas, since the testing part requires only Eigen vectors and mean values, as shown in Figure. 4(a) [19], therefore in case of PCA the computed mean and  $E_v$  for  $D_i$  are pre-stored in the flash memory of the board and at run-time the hardware will take those values to perform normalization and projection of  $D_i$  with lower complexity and faster speed.

In contrast to PCA, LDA is not performed directly on  $D_i$  because LDA deals with class boundaries which cannot be identified in  $D_i$ . Therefore,  $D_i$  is split in to classes such that data for each gas is considered as a single class. The training-data obtained at different concentrations of gas is stored as a train-class ( $T_c$ ), where sub-script  $c$  is representing the type of gas. After computing normalization as well as between and within class-differences, the  $E_v$  will be computed. The  $E_v$  is then forwarded to the projection block which projects the  $D_i$  on reduced feature space. It is worth noticing that LDA testing part requires only Eigen vectors as shown in Figure. 4(b) to project  $D_i$  on reduced feature space.

C. Classification

A Binary Decision Tree (BDT) classifier is used to identify the gases after feature reduction. The reason of selecting BDT for classification is because of the simplicity and good performance. The tree formation is carried out on  $D_i$  using MATLAB library function whereas the decision nodes will be implemented on hardware using successive if-else condition to classify the gases at run-time from the obtain  $D_i$ .

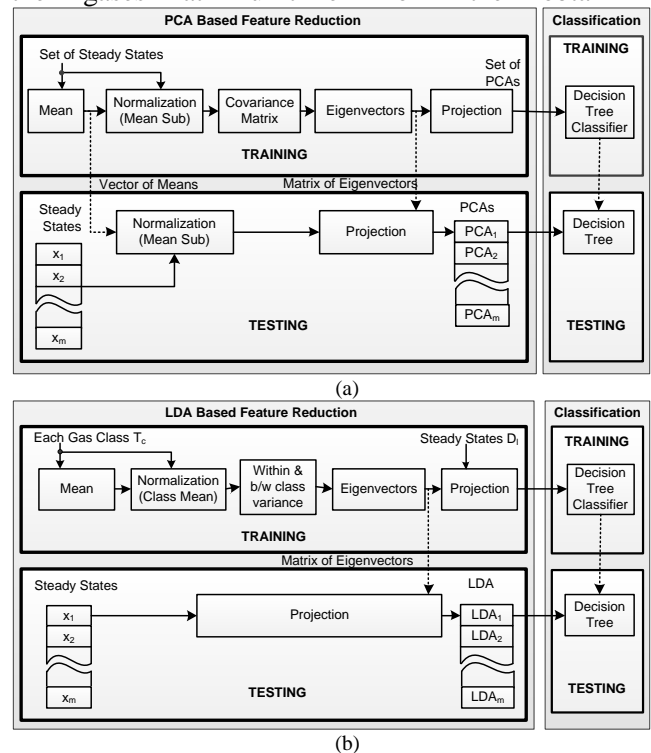


Figure 4. Feature reduction algorithm based on (a) PCA and (b) LDA

V. IMPLEMENTATION RESULTS OF THE PROCESSING UNIT

The software simulation is carried out using MATLAB whereas the hardware implementation is achieved using Vivado HLS tools [21]. It has been observed that for classification BDT with three principal components can classify 90% of gases [19] and is therefore 7% better than using LDA based feature reduction.

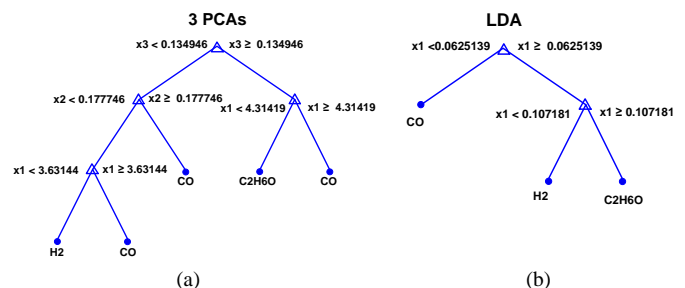


Figure 5. BDT for (a) PCA and (b) LDA

TABLE I. SIMULATION RESULTS FOR GAS-CLASSIFICATION AND HARDWARE OVERHEAD WITH PCA/LDA BASED FEATURE REDUCTION

Properties		LDA	PCA	
			2-PCA	3-PCA
Classification	Steady State (SS)	83%	80%	90%
	FF	893	2089	2089
Hardware Resources	LUT	1937	3925	3925
	Clock Cycles (CC) (Nano-seconds) ns	8.20	8.20	8.20
	Latency Period (CC)	163	261	261
	Input Interval (CC)	164	262	262

However, for hardware implementation LDA based feature reduction requires 50% less Look Up Tables (LUTs) and 57% less Flip-Flops (FF) than PCA. Moreover, LDA requires 37.5% less latency time than PCA. Where latency time is the period require to produce the final output, as shown in Table. I.

Furthermore, the BDT obtained with LDA based feature reduction algorithm exhibits only 2 decision nodes along with unity depth, while in case of PCA the BDT have 4 decision nodes with three steps in depth. Therefore, LDA offers simplified decision tree which require less time for searching and classification of gas than PCA, as shown in Figure. 5.

VI. CONCLUSION

Since the reader is considered as a key component of the RFID gas application system, therefore a UHF RFID reader is presented with a processing unit implemented on a reconfigurable Zynq platform. The overview of the reader performance characterization is also demonstrated. Whereas, ongoing research focuses on the design and implementation of efficient reconfigurable architectures for OMP algorithm The RFID system is compliant with the EPC-Gen2 protocol in the 902-928 MHz ISM frequency band. ThingMagic embedded M6e reader shows an advantage over existing readers in the market in term of high integration, low power dissipation and low cost.

The designed processing unit at reader is tested with PCA and LDA based feature reduction approaches. It is found that BDT can classify 90% of the gases with three principal components which is 7% more efficient than the identification of gas by BDT using LDA. While in terms of hardware overhead LDA requires 50% less LUTs than PCA and is 37.5% more efficient in terms of latency time.

The presented work is part of an ongoing project in which a low-power multi-sensing gas identification platform is need to be developed for gas identification based on an array of tin-oxide gas sensors. Therefore the system will be tested on real conditions after the completion of the integration process.

ACKNOWLEDGMENT

This paper was made possible by National Priorities Research Program (NPRP) grant No. 5 – 080 – 2 – 028 from the Qatar National Research Fund (a member of Qatar Foundation). The statements made herein are solely the responsibility of the authors.

REFERENCES

- [1] N. Yamazoe, and N. Miura, "Environmental gas sensing", *Sensors and Actuators B: Chemical*, vol. 20, no. 2-3, 1994, pp. 95-102.
- [2] S. Labreche, S. Bazzo, S. Cade, and E. Chanie, "Shelf life determination by electronic nose: application to milk", *Sensors and Actuators B: Chemical*, vol. 106, no. 1, 2005, pp. 199-206.
- [3] S. Dragonieri et al. "An electronic nose in the discrimination of patients with asthma and controls", *Journal of Allergy and Clinical Immunology*, vol. 120, no. 4, 2007, pp. 856-862.
- [4] F. Röck, N. Barsan, and U. Weimar, "Electronic nose: current status and future trends", *Chemical reviews*, vol. 108, no. 2, 2008, pp. 705-725.
- [5] M. Shi, A. Bermak, S. B. Belhouari, and P.C. Chan, "Gas identification based on committee machine for microelectronic gas sensor", *IEEE Transactions on Instrumentation and Measurement*, vol. 55, no. 5, 2006, pp. 1786-1793.
- [6] B. Guo, A. Bermak, P.C. Chan, and G.Z. Yan, "An Integrated Surface Micromachined Convex Microhotplate Structure For Tin Oxide Gas Sensor Array", *IEEE Sensors Journal*, vol. 7, no. 12, 2007, pp. 1720-1726.
- [7] E. Llobet et al. , "Multicomponent gas mixture analysis using a single tin oxide sensor and dynamic pattern recognition", *IEEE Sensors Journal*, vol. 1, no. 3, 2001, pp. 207-213.
- [8] L. Yang, R. Zhang, D. Staiculescu, C. P. Wong, and M. M. Tentzeris, "A novel conformal RFID-enabled module utilizing inkjet-printed antennas and carbon nanotubes for gas-detection applications", *Antennas and Wireless Propagation Letters, IEEE*, vol. 8, 2009, pp. 653-656.
- [9] M. Brandl et al. "A low-cost wireless sensor system and its application in dental retainers", *IEEE Sensors Journal*, vol. 9, no. 3, 2009, pp. 255-262.
- [10] S. Mohamad, F. Tang, A. Amira, A. Bermak, and M. Benammar, "A Low Power Oscillator Based Temperature Sensor For RFID Applications", *5th Asia Symposium on Quality Electronic Design (ASQED)*, 2013, pp. 50-54.
- [11] H. Rabah, A. Amira, B. K. Mohanty, and S. Almaadeed, "FPGA Implementation of Orthogonal Matching Pursuit for Compressive Sensing Reconstruction", *IEEE Transactions on Very Large Scale Integration Systems* , DOI: [10.1109/TVLSI.2014.23358716](https://doi.org/10.1109/TVLSI.2014.23358716) .
- [12] R. Weinstein, "RFID: A Technical Overview and it's Application to the Enterprise," *IT Professional*, vol. 7, no. 3, 2005, pp. 27-33.
- [13] EPCglobal Inc., "EPC Radio-Frequency Identity Protocols Class-1 Generation-2 UHF RFID Protocol for Communications at 860MHz-960MHz Version 1.0.9", *EPC global Standards*, 2005.
- [14] K. Finkenzeller, "RFID Handbook", New York: Wiley, 2003.
- [15] A. S. Ahson, and M. Ilyas, "RFID Handbook: Applications, Technology, Security, and Privacy", *CRC Press*, 2008.
- [16] P. Nikitin, K. V. S. Rao, and S. Lam, "UHF RFID tag characterization: overview and state-of-the-art", *Antenna Measurement Techniques Association Symposium (AMTA) 34th Annual Meeting and Symposium*, 2012, pp. 289-294.

- [17] M. Zgaren, and M. Sawan, "A Front end-EPC Gen-2 Passive UHF RFID Transponder for Embedded Gas Sensor", 4th International Gas processing symposium, 2014, pp. 223-231.
- [18] 'M6e High-Performance 4-Port UHF RFID Module', [http://www.dpie.com/manuals/rfid/M6eHardwareGuide\\_Sept13.pdf](http://www.dpie.com/manuals/rfid/M6eHardwareGuide_Sept13.pdf), v 1.13.1, accessed May. 12,2015.
- [19] A. Ait Si Ali, A. Amira, F. Bensaali, and M. Benammar, "Hardware PCA for Gas Identification Systems Using High Level Synthesis On The Zynq SoC", IEEE 20th International Conference on Electronics, Circuits, and Systems (ICECS) , 2013, pp. 707-710.
- [20] 'Inc Xilinx. Zynq-7000 All Prog. SoC: Tech. Reference Manual', [http://www.xilinx.com/support/documentation/user\\_guides/ug585-Zynq-7000-TRM.pdf](http://www.xilinx.com/support/documentation/user_guides/ug585-Zynq-7000-TRM.pdf), UG585, v1.8.1, accessed Feb. 20, 2015.
- [21] 'Inc Xilinx Vivado Design Suite User Guide: Embedded Processor H/W Design', [http://www.xilinx.com/support/documentation/sw\\_manuals/xilinx2013\\_3/ug898-vivado-embedded-design.pdf](http://www.xilinx.com/support/documentation/sw_manuals/xilinx2013_3/ug898-vivado-embedded-design.pdf), UG898, v2014.3, accessed March 9, 2015.